

Microwave synthesis and the characterization of Sm^{3+} -doped laser absorber

YUANYAO LI*, TIEGEN LIU, YANG DU

Optical Engineering, College of Precision Instrument and Optoelectronics Engineering, Tianjin University, Tianjin 300072, China

A very high efficiency method using microwave heating to synthesize Sm^{3+} doped ultra-fine (sub-micro) powder is shown in this paper. We studied the absorption spectrum of the powder, and we find that there are many absorption peaks. Based on the absorption property of this powder, we make a laser protection coating at 9398 cm^{-1} . The coating reduced the reflected light power by 89% compare to the one without coating. This shows that the as-prepared ultra-fine powder has great potentials in many aspects such as laser protective coatings, anti-counterfeiting inks and so on.

(Received June 21, 2011; accepted July 25, 2011)

Keywords: Spectroscopy, Optical materials and properties, Rare-earth-doped materials, Microwaves

1. Introduction

Rare earth (RE) metals, with unique structures of electronic shells and excellent properties, are the 57th to 71th elements in the periodic table of chemical elements [1]. The 4f shell of the RE ions are shielded by the $5s^25p^2$ orbitals and the influence of the surrounding on the electronic transitions within the 4fⁿ configuration is hence small. Consequently, the optical transitions yield sharp lines in the optical spectra and long decay time of the excited states [2, 3]. Despite of these facts, the luminescence of the RE ions is widely used in several commercial applications, for instance laser glasses, fiber amplifier, optical glasses and so on [4-8]. However, those are all focusing on the frequency conversion properties and emission spectrum of RE ions, few of them talked about the absorption spectrum and applications.

In this paper, we synthesized ultra-fine powders with strong laser absorption at some specific wave numbers by microwave heating [9, 10]. Compare to traditional ways, this is a new chemical synthesis method with the nature of quicker reaction speed, lower reaction temperature as well as smaller particle size [11-14]. And based on the absorption property of them, these powders synthesized can be used in many fields such as laser protection, anti-counterfeiting.

2. Experiments

Fig. 1 gives the microwave synthesis apparatus we employed in this experiment. The starting materials of SiO_2 (99.9% purity), PbF_2 (99.9% purity) and Sm_2O_3 (99.99% purity) etc. were put into a corundum crucible in proportion. In order to improve the uniformity of heating and to preserve the heat inside the crucible, we introduced a bigger graphite crucible to cover it. The graphite also plays a role of microwave susceptor to accelerate heating. The gap between the two crucibles we filled with quartz

sand. And then, we placed the graphite crucible into an aluminosilicate container with the gap filled with quartz sand too. Afterwards, the aluminosilicate container was heated in a microwave oven at a power of 800 W and a frequency of 2.45 GHz. Experimental conditions for the samples and their morphologies are shown in Table 1.

3. Results and discussion

Fig. 2 presents the X-Ray diffraction (XRD) patterns of the samples. The data were recorded at room temperature on Rigaku D/max 2500v/pc with Bragg-Brentano geometry using $\text{Cu K}\alpha 1$ radiation $\lambda=1.5406\text{ \AA}$. According to the analysis of XRD patterns, except some excess reactants, Sm^{3+} ions exist in the form of fluoride, such as SmF_3 (PDF 12-0792) and SmOF (PDF 89-0458, ICSD 81948) in all samples.

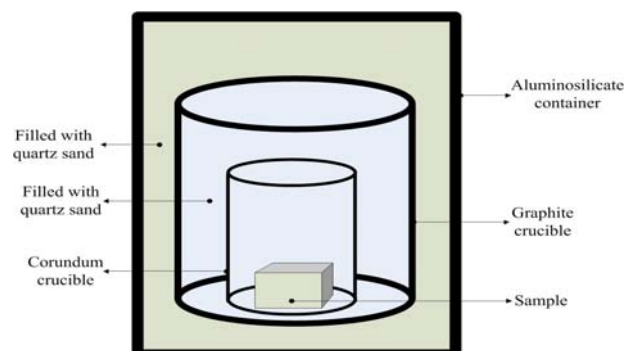


Fig. 1. The device of microwave heating.

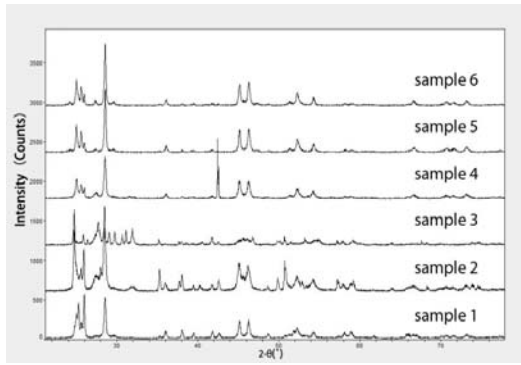


Fig. 2. XRD profiles of sample 1 to 6.

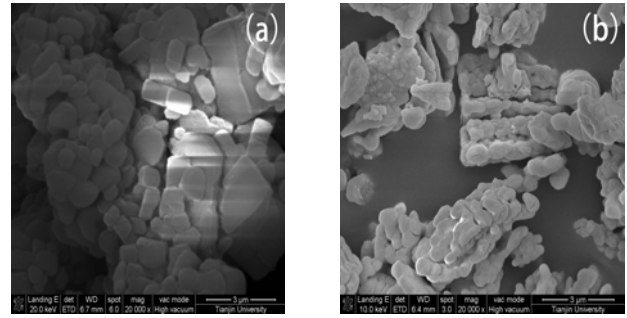


Fig. 3. SEM micrographs of sample 2: (a) and sample 5: (b).

Table 1. Experimental conditions for the samples and their morphologies.

Sample No.	Concentration of Sm ₂ O ₃ (wt.%)	Heating time(min)	Morphology
1	20%	10	Rectangular
2	35%	10	Rectangular
3	60%	10	Rodlike
4	60%	20	Rodlike
5	60%	30	Rodlike
6	60%	40	Rodlike

Table 2. Observed and theoretical energy levels of Sm³⁺ in cm⁻¹.

Main component	E _{obsd}						E _{theo}
	Card 1	Card 2	Card 3	Card 4	Card 5	Card 6	
⁶ H _{5/2} → ⁶ F _{11/2}	10598	10598	10575	10598	10560	10556	10471
⁶ H _{5/2} → ⁶ F _{9/2}	9187	9187	9160	9191	9187	9187	9090
⁶ H _{5/2} → ⁶ F _{7/2}	8060	8060	7987	8060	8060	8060	7931
⁶ H _{5/2} → ⁶ F _{5/2}	7185	7185	7185	7185	7185	7185	7085
⁶ H _{5/2} → ⁶ F _{3/2}	6718	6718	6633	6726	6718	6718	6596
⁶ H _{5/2} → ⁶ H _{15/2}		6633	6518		6433	6429	6462
⁶ H _{5/2} → ⁶ F _{1/2}	6417	6398	6390		6363	6356	6351

The morphologies of samples, investigated by a field emission scanning electron microscope (FESEM, NOVA NanoSEM 430), are present in Table 1. Fig. 3 shows the SEM photos of sample 2 and 5.

As illustrated in Fig. 3, particles are agglomerated more and more closely with increasing the contentment of Sm₂O₃, respectively, the morphologies change from rectangular to rodlike. All samples are well crystallized with a particle size of less than 1µm in general. It is interesting that the particles do not aggregate randomly, but grow along one direction, thereby come out the rodlike morphology.

Then we placed the samples on 6 foil sheets separately, named card 1 to 6 corresponding to the former samples. Fig. 4 shows the reflection profiles of them (obtained by Nicolet Antaris FT-NIR Analyzer) with wave numbers varying from 6000 cm⁻¹ to 9500 cm⁻¹. The majority of the electronic transitions between the free ion ^{2S+1}L_J levels of Sm³⁺ originate from the electric dipole (ED) interactions with the ΔJ≤6 selection rule. However, contribution from the magnetic dipole (MD) interaction with the ΔJ=0, ±1 selection rule cannot be neglected. The J-mixing by the crystal field (CF) effect lifts partially the restrictions imposed by the free ion selection rules.

According to Beer-Lambert law, it can be observed that the absorption peaks of Sm³⁺, originating from the absorption from the ground state ⁶H_{5/2} to ⁶F_{1/2-11/2} and ⁶H_{15/2}, are enhanced with the increase of the rare earth content while no significant changes arise in the center of the absorption spectra. This absorption enhancement is expressed as the decline in reflectivity from card 1 to card 3 in Fig. 4 (a) as well. Fig. 4 (a) also indicates that there are partially overlaps in states ⁶F_{1/2-11/2} and ⁶H_{15/2} and the theoretical sharp absorption peaks of Sm³⁺ is broadened on both sides with a different spreading as the Sm₂O₃ concentration increases. This inhomogeneous broadening can be put down to the fact of Stark splitting. Since the outer electron of RE ions shields the 4f shell imperfectly, the surrounding ligand field can still make the energy level of Sm³⁺ split into a series of Stark levels, particularly when the Sm₂O₃ content is very high. The interactions between RE ion and ligand field and among RE ions are then strengthened, resulting in the splitting in the energy levels and inhomogeneous broadening of the characteristic absorption peaks of Sm³⁺.

Fig. 4(b) shows that the reflectance first decreases (from card 3 to 4) as heating time prolonged and then increases (from card 4 to 6). The possible reason is that

with the increase of heating time, more Sm^{3+} ions enter into the lattice of raw stuff, causing a decline in reflectance. Nevertheless, longer heating time, meaning higher temperature, makes more raw materials with low boiling point into gas, taking several Sm^{3+} ions which are already in their lattices away, and then less Sm^{3+} left in the powder, which manifests a slight rise in reflectivity in Fig. 4 (b).

The exact absorption centers are present in table 2. In contrast with the theoretical values, they shifted to larger wave numbers in all the samples (Fig. 4). This blue shift can be expressed as the formula proposed by Brus[15]:

$$\Delta E = \frac{h^2 \pi^2}{2R^2} \left(\frac{1}{m_e} + \frac{1}{m_h} \right) - \frac{1.786e^2}{4\pi\epsilon_\infty\epsilon_0 R} + \text{smaller terms}$$

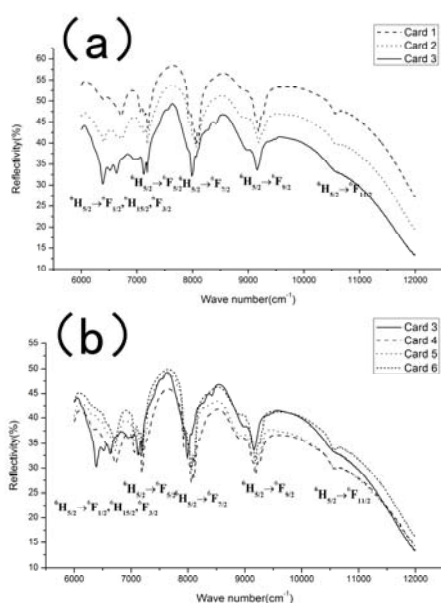


Fig. 4. Reflection profiles of (a): card 1(dash), card 2(dot) and card 3(solid), and (b): card 3(solid), card 4(dash), card 5(dot) and card 6(short dash).

where m_e and m_h are the effective mass of electrons and holes, ϵ_0 and ϵ_∞ are the dielectric constant of vacuum and high-frequency, h is the Planck constant and R is the particle radius. With the particle size decreases to the magnitude of nanometer, the absorption center gradually blue shifts. According to the position of absorption center, we can see that the particle size decreases (from card 1 to card 3) with the Sm_2O_3 content increases in the same heating time. However the particle size will decrease and then increase (from card 3 to card 6) as the heating time prolonged with the same Sm_2O_3 content. In order to make the most effective laser absorption powder at 9398 cm^{-1} (1064 nm), considering the theoretical absorption center of ${}^6\text{H}_{5/2} \rightarrow {}^6\text{F}_{9/2}$ is 9090 cm^{-1} , we have to maximize the blue shift and minimize reflectance, so the best synthesis condition is heating 20 min with 60 wt.% Sm_2O_3 doped

In order to test the powder's property of laser protection in practical cases, we mixed the sample 4 with painting and coated it (0.1mm thick) on an aluminium alloy plate (1m^2 square) and then measured its reflected

light power at 9398 cm^{-1} with the optical power meter (Thorlabs S122C). The power reflected with coating on the plate is -17.2 dBm, compared to -10.61 dBm which was the reflected light power of the plate without coating, meaning the power had decreased 89%. This implies the as-prepared coating has great potential in laser protection at this wave number.

4. Conclusion

In conclusion, we have synthesized ultra-fine powders with low reflectance at several wave numbers (e.g. 9398cm^{-1}) by microwave heating. The optimized synthesis condition for the powder is heated 20 min with content of 60% of Sm_2O_3 in weight. By mixing the powders with liquid or solids, we can transplant the property of strong absorption at these special wave numbers to them. Laser protection coating is one of the best examples. The as-prepared protection coating can reduce the reflectance with 89% at 9398cm^{-1} . These findings have implications for the fields of laser protection and anti-counterfeiting. The attainments of lower reflectivity and smaller particle size are still elusive and challenging, and performing as the focuses of our future work.

References

- [1] W. He, J. Zhang, L. Wang, Q. Zhang, J. Rare Earth **27**, 231 (2009).
- [2] Z. Siyuan, Spectroscopy of rare earth ions. Science Press, Beijing (2008).
- [3] J. Hölsä, E. Säilynoja, P. Ylhä, P. Porcher, P. Dereñ, W. Streck, J. Phy. Chem. **100**, 14736 (1996).
- [4] Y. Kawamoto, R. Kanno, J. Qiu, J. Mater. Sci **33**, 63 (1998).
- [5] F. I. Vasile, P. Schiopu, J. Optoelectron. Adv. M. **6**, 1207(2004).
- [6] H. Ma, S. Xu, J. Mater. Sci. **41**, 3155 (2006).
- [7] Z. Xia, H. Du, J. Sun, J. Optoelectron. Adv. M. **12**, 975(2010)
- [8] S. Zhang, B. Zhu, S. Zhou, S. Xu, J. Qiu, Opt. Express **15**, 6883 (2007).
- [9] Y. Bykov, K. Rybakov, J. Phys. D: Appl. Phys. **34**, 55 (2001).
- [10] K. J. Rao, B. Vaidhyanathan, M. Ganguli, Pa. Ramakrishnan, Chem. Mater. **11**, 882 (1999).
- [11] J. Ryu, J. Yoon, K. Shim Solid State Commun **133**, 657 (2005).
- [12] A.-M. Chinie, A. Stefan, S. Georgescu, O. Toma, E. Borca, M. Bercu, J. Optoelectron. Adv. M. **8**, 95(2006).
- [13] D. Ravichandran, S. T. Johnson, S. Erdei, R. Roy, W. B. White Displays **19**, 197 (1999).
- [14] H. Schäfer, P. Ptacek, B. Voss, H. Eickmeier, Jr Nordmann, M. Haase Cryst Growth Des **10**, 2202 (2010).
- [15] L. Brus J. Phy. Chem. **90**, 2555 (1986).

*Corresponding author: liyuanyao1984@163.com